Published in final edited form as:
Multimodal Brain Image Anal (2013). 2013 ; 8159: 84–94. doi:10.1007/978-3-319-02126-3_9.

Mapping Dynamic Changes in Ventricular Volume onto Baseline Cortical Surfaces in Normal Aging, MCI, and Alzheimer's Disease*

Sarah K. Madsen[1], **Boris A. Gutman**[1], **Shantanu H. Joshi**[2], **Arthur W. Toga**[1], **Clifford R. Jack Jr.**[3], **Michael W. Weiner**[4,5], and **Paul M. Thompson**[1]

[1]Imaging Genetics Center, Laboratory of Neuro Imaging, UCLA School of Medicine, Los Angeles, CA 90095, USA

[2]Laboratory of Neuro Imaging, UCLA School of Medicine, Los Angeles, CA 90095, USA

[3]Mayo Clinic, Rochester, MN, USA

[4]Departments of Radiology, Medicine, Psychiatry, UC San Francisco, San Francisco, CA, USA

[5]Department of Veterans Affairs Medical Center, San Francisco, CA, USA

Abstract

Ventricular volume (VV) is a powerful global indicator of brain tissue loss on MRI in normal aging and dementia. VV is used by radiologists in clinical practice and has one of the highest obtainable effect sizes for tracking brain change in clinical trials, but it is crucial to relate VV to structural alterations underlying clinical symptoms. Here we identify patterns of thinner cortical gray matter (GM) associated with dynamic changes in lateral VV at 1-year (N=677) and 2-year (N=536) intervals, in the ADNI cohort. People with faster VV loss had thinner baseline cortical GM in temporal, inferior frontal, inferior parietal, and occipital regions (controlling for age, sex, diagnosis). These findings show the patterns of relative cortical atrophy that predict later ventricular enlargement, further validating the use of ventricular segmentations as biomarkers. We may also infer specific patterns of regional cortical degeneration (and perhaps functional changes) that relate to VV expansion.

Keywords

imaging biomarkers*; brain imaging; magnetic resonance imaging; quantitative image analysis; statistical analysis; temporal/longitudinal image series analysis

1 Introduction

The lateral ventricles are a fluid-filled region within the brain that expands to fill space formerly occupied by degenerating brain tissue inside the fixed volume of the skull. Ventricular volume (VV) is a widely-used biomarker of Alzheimer's disease (AD)

*For the Alzheimer's Disease Neuroimaging Initiative (ADNI).

progression; it offers one of the highest effect sizes for tracking brain change over time, and for detecting disease effects, making it highly advantageous in clinical trials.

Clinically, VV is commonly used by radiologists to help diagnose neurodegeneration, more so than many of the more complex brain MRI measures analyzed in research. Even so, information is sorely needed on what VV changes imply in terms of alterations in regions underlying cognitive functions, such as the cortex. Cross-structure correlations linking changes in VV to differences in other brain tissues have been largely ignored in univariate analyses of single structures or maps.

Reductions in gray/white matter contrast with age make it challenging to detect longitudinal change in many brain structures - such as the hippocampus and cortex - usually requiring time-consuming manual edits even with the most widely-used segmentation packages. In contrast, the boundary demarcating the lateral ventricles (cerebrospinal fluid (CSF)/brain tissue) is easier to detect, making ventricular segmentation reliable and robust [1]. As brain atrophy progresses, changes in cortical structure become even more extreme, along with further reductions in contrast at the gray/white interface. Segmentation of cortical structures, which tend to have greater functional significance, becomes even more difficult in the aging population.

The lateral ventricles can be measured in brain MRI scans using several different techniques. VV [7], shape [2], and boundary shift integral [8] have been validated as highly sensitive biomarkers of AD and mild cognitive impairment (MCI), offering high classification accuracy and greater consistency than some cognitive tests [9], [10]. Longitudinal studies show that VV is a very sensitive biomarker of ongoing atrophy in elderly populations. In elderly non-demented adults, VV changes at a markedly faster rate (2.80–4.4% per year) than hippocampal volumes (0.68–0.84% per year) [3]. Changes in VV may be faster in MCI and earlier AD than in later AD or normal aging [7], [11], but accumulated VV differences are most extreme in later stages of AD [12].

Prior methods for VV segmentation have used semi-automated, automated [4], and single-atlas or multi-atlas methods [5]. In this analysis, we segmented the ventricles with a modified multi-atlas approach. Our segmentation method makes use of group-wise surface registration of existing templates, and applies surface-based template blending for more accurate results [5]. For cortical segmentation, we use the standard FreeSurfer tools (v5.0.0) [6].

Most studies of VV have been univariate, looking at the ventricles alone as a single structure, which does not allow more detailed interpretations of how changes in VV relate to other brain regions. Two groups have related VV to shape and volume differences in periventricular brain structures (including the hippocampus) [1], [2]; however, as far as we know, ours is the first study to use VV to infer cortical brain structure differences. By inferring cortical alterations from ventricular changes, we can better interpret results of clinical trials that show a deceleration in the rate of VV loss.

2 Methods

2.1 Cohort Studied

We analyzed 677 individuals who had received a high-resolution, T1-weighted structural MRI brain scan as part of phase 1 of the Alzheimer's Disease Neuroimaging Initiative (ADNI1) and whose scans passed quality control for both ventricular and cortical segmentations. Segmentations were assessed visually from multiple views for defects. All subjects passed quality control (QC) for ventricle segmentations and six subjects were excluded during QC of cortical GM surfaces.

ADNI is a multi-site, longitudinal study of patients with Alzheimer's disease (AD), individuals with mild cognitive impairment (MCI) and healthy elderly controls (HC). Standardized protocols maximize consistency across sites.

2.2 Scan Acquisition and Processing

For VV segmentation, we analyzed baseline, 1-year (N=677), and 2-year (N=536) follow-up brain MRI scans (1.5-Tesla, T1-weighted 3D MP-RAGE, TR/TE = 2400/1000 ms, flip angle = 8°, slice thickness = 1.2 mm, final voxel resolution = $0.9375 \times 0.9375 \times 1.2\ mm^3$). Raw MRI scans were pre-processed to reduce signal inhomogeneity and were linearly registered to a template (using 9 parameters).

For cortical GM segmentation, we analyzed 677 baseline brain MRI scans (1.5-Tesla, T1-weighted 3D MP-RAGE, TR/TE = 2400/1000 ms, flip angle = 8°, slice thickness = 1.2 mm, 24-cm field of view, a 192×192×166 acquisition matrix, final voxel resolution = $1.25 \times 1.25 \times 1.2\ mm^3$, later reconstructed to 1 mm isotropic voxels). To simplify the presentation, we did not perform cortical segmentation at later time points, as the baseline differences tend to reflect the overall level of atrophy, and to some extent they also reflect the rate of atrophy.

Bias field correction (N3) was applied as part of the standard ADNI dataset preprocessing before scans were downloaded. We used a registration with 9 parameters as it corrects for scanner voxel size variation and arguably outperforms 6 parameter registration in multi-site studies such as ADNI [13], [14]. Independent alignment procedures were used for the ventricles and for the cortex, as described below (**Sections 2.3 and 2.4**), using methods optimized for each structure.

2.3 Ventricular Segmentation

Ventricular segmentation was performed using a validated method [15]. Ventricular surfaces were extracted using an inverse-consistent fluid registration with a mutual information fidelity term to align a set of hand-labeled ventricular templates to each scan. The template surfaces were registered as a group following a medial-spherical registration method [15]. To improve upon the standard multi-atlas segmentation, which generally involves a direct, or a weighted average of the warped binary masks, we selected an individual template that best fits the new boundary at each boundary point. A naïve formulation of this synthesis can be written as below:

(1)

Here, I, S are the new image and boundary surface, $\{I_i, T_i\}_i$ are template surfaces and images warped to the new image, and $s(I, I_i)[p]$ is some local normalized similarity measure at point p. Normalized mutual information around a neighborhood of each point was used as similarity. This approach allows for more flexible segmentation, in particular for outlier cases. Even a weighted average, with a single weight applied to each individual template, often distorts geometric aspects of the boundary that are captured in only a few templates, perhaps only in one. However, to enforce smoothness of the resulting surface, care must be taken around the boundaries of the surface masks W^i. An effective approach is to smooth the masks with a spherical heat kernel, so that our final weights are

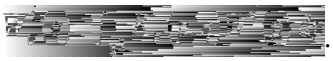

.

2.4 Cortical Segmentation

Cortical reconstruction and volumetric segmentation were performed with the FreeSurfer (v5.0.0) image analysis suite, which is freely available online (http://surfer.nmr.mgh.harvard.edu/). Details of these procedures have been described previously [6]. Briefly, the processing includes removal of non-brain tissue, intensity normalization, tessellation of the cortical gray/white matter boundary, automated topology correction and surface deformation along intensity gradients to optimally define cortical surface borders, registration to a spherical atlas using individual cortical folding patterns to align cortical anatomy across individuals, and creation of 3D maps of GM (as measured with thickness, volume, and surface area) at each cortical surface point. After processing, images are in an isotropic space of 256 voxels along each axis (x, y, and z) with a final voxel size of 1 mm^3.

2.5 Statistical Analysis: Mapping Ventricular Change onto the Cortical Surface

Statistical tests were conducted at each point on the cortical surface separately for 1-year and 2-year change in VV after applying cortical smoothing (kernel radius=25 mm, full width at half maximum). We tested a series of general linear models (GLM) of change in VV on cortical GM thickness after: (1) controlling for effects of sex, age, and diagnosis (AD, MCI, or healthy elderly controls) in all individuals (1-year change: N=677; 2-year change: N=536), (2) controlling for sex and age in AD, MCI and control groups, separately (1-year: AD N=142, MCI N=335, Control N=200; 2-year: AD N=109, MCI N=251, Control N=176), and (3) controlling for sex and age in matched groups of N=100 AD, MCI and controls. Analyses were run separately for associations within each hemisphere (i.e., for change in left VV with left cortical GM thickness and for right VV change with right cortical GM thickness). To control the rate of false positives, we enforced a standard false discovery rate (FDR) correction for multiple statistical comparisons across voxels in the entire left and right brain surfaces, using the conventionally accepted false positive rate of 5% (q=0.05) [16].

2.6 *Post Hoc* Statistical Analysis: Linear Relationships between Regional Cortical Thickness and Ventricular Change

We identified clusters that passed FDR in the 3D cortical surface maps for the matched groups of N=100 AD, MCI, and controls for the GLM of 2-year change in VV on cortical GM thickness after controlling for sex and age. Within each statistically significant cluster on the cortical surface, we calculated mean cortical GM thickness for each subject. We then plotted each subject's mean cortical GM thickness and raw 2-year change in VV for each group (AD, MCI, and controls for N=100), to understand the characteristics (i.e., magnitude and shape) of the significant associations we found in our surface GLM between the two measures.

3 Results

In the full sample, we found that (Figure 1) 1-year (N=677) and 2-year (N=536) changes in VV were significantly associated with baseline cortical GM thickness in temporal, inferior and anterior frontal, inferior parietal, and some occipital regions, after controlling for age, sex, and diagnosis. The significant regions were somewhat more expansive, in the same areas, for the 2-year change compared to the 1-year change in VV. If ventricular change is linear, these two maps should be the same, but the 2-year map may show more extensive or stronger associations because the 2-year measures have greater SNR. All results presented pass a hemispheric FDR correction at q=0.05.

Looking separately at diagnosis (Figure 2), 1-year and 2-year changes in VV were most strongly associated with baseline cortical GM thickness in MCI, with maps similar to those for the full cohort. In MCI, left inferior and anterior frontal, temporal, inferior parietal, and inferior occipital regions were significantly negatively associated with 1-year change in VV (left: $-\log_{10}(p\text{-values})$=1.58–3.84, right: $-\log_{10}(p\text{-values})$=3.28–5.54, corrected). Somewhat larger regions, bilaterally, were significantly negatively associated with 2-year change in ventricular volume in MCI (left: $-\log_{10}(p\text{-values})$=1.55–3.81, right $-\log_{10}(p\text{-values})$=1.55–3.80, corrected). In AD, significant negative associations were found in the bilateral superior frontal, left middle frontal, and left anterior and posterior cingulate cortex for 1-year change in VV (left: $-\log_{10}(p\text{-values})$=2.39–4.64, right: $-\log_{10}(p\text{-values})$=3.04–5.30, corrected). Significant negative associations for 2-year change in VV were found in left anterior and posterior cingulate cortex and small clusters in the left superior and middle frontal cortex for AD (left: $-\log_{10}(p\text{-values})$=2.95–5.20, right: $-\log_{10}(p\text{-values})$=3.64–5.90, corrected). In elderly controls, right superior frontal GM thickness at baseline was significantly negatively associated with 2-year change in VV (right: $-\log_{10}(p\text{-values})$=3.32–5.582, corrected); no significant associations were detected for 1-year change, perhaps because SNR for tracking change is poorer when the interval is shorter, especially in this group which is expected to have slower rates of VV expansion.

In MCI, longitudinal changes in VV are associated with cortical GM thickness in a well-known pattern of areas vulnerable to AD pathology [17], [18], such as progressive accumulation of beta-amyloid that precedes cognitive decline and tau that parallels cognitive decline, as measured by F18-FDDNP PET brain scans (Figure 3). Primary sensorimotor areas that are spared in AD, which are also difficult to segment due to very thin GM and

overabundance of myelin creating poor tissue contrast in MRI, were not significant in our maps.

To examine if insufficient power contributed to differences in results for groups with smaller sample size, we re-analyzed subsets of N=100 matched by age and sex in the AD, MCI, and control groups at 1-year and 2-years. In the equally-sized subsets, 1-year change in VV was negatively associated with right superior frontal cortex thickness in AD (left: not significant, right: $-\log_{10}(p\text{-values})=3.66–5.92$). No other significant results were found for 1-year change in VV for MCI or elderly controls with N=100. Two-year change in VV (Figure 4**, top panel**) was negatively associated with GM thickness in left posterior and rostral anterior cingulate, lateral orbitofrontal, and rostral middle frontal cortex in AD (left: $-\log_{10}(p\text{-values})=2.15–4.41$, right: not significant) and left pars orbitalis, fusiform, the isthmus and posterior cingulate, and superior frontal cortex in MCI (left: $-\log_{10}(p\text{-values})=2.15–4.41$, right: not significant). In elderly controls, 1-year change in VV was negatively associated with GM thickness in the right insula, superior frontal, precuneus, supramarginal, transverse temporal, inferior parietal, and isthmus of the cingulate cortex (left: not significant, right: $-\log_{10}(p\text{-values})=2.28–4.54$).

After limiting the sample size of all groups to N=100 (the approximate size of the smallest group), the extent of significant regions appears roughly similar across groups, supporting the interpretation that the more prominent effects seen in the full-sized MCI sample (twice as large as the other groups) may be attributed to increased power rather than specific to this diagnostic category.

To better understand the characteristics of the relationship we found between VV and GM thickness in the surface GLMs (Figure 4**, top panel**), we plotted raw 2-year change in VV against mean GM thickness at baseline (averaged across all surface points within distinct statistically significant regions from the surface GLMs) in each subject from the N=100 subsets for AD, MCI, and CON (Figure 4**, bottom panel**). As expected, all plots show negative relationships (greater VV expansion over time is associated with thinner baseline GM). Plots for AD (top row of plots) and MCI (second and third rows of plots) show greater variance and higher rates of expansion in 2-year VV compared to healthy elderly controls (bottom two rows of plots) for all statistical regions of interest. The plots also show that elderly controls have higher baseline GM thickness in several regions compared to AD and MCI groups. Steeper slopes for the healthy elderly control group may be explained by greater variance in baseline GM thickness compared to AD and MCI groups.

4 Discussion

Our results complement the current literature on change in ventricular enlargement as a robust clinical biomarker of disease progression in the early stages of AD. We also make a novel contribution to the field, which has largely ignored cross-structural correlations with VV, by showing how changes in VV relate to cortical GM thickness in normal aging and in varying stages of Alzheimer’s dementia. These results allow us to make stronger inferences about functionally important areas of the cortex, based on ventricular segmentations.

The cortical regions significantly associated with dynamic changes in VV are among those that are regarded as most susceptible to AD-related pathologies in multiple domains, including accumulation of amyloid plaques and tau neurofibrillary tangles, metabolic disruption, functional and connectivity alterations, and structural GM loss. Interestingly, the lateralization of our findings (left in AD and MCI, right in controls) may not hold up in larger samples with higher statistical power. In equally-sized samples the extent of significant associations was similar across groups.

Ventricular measures on MRI are among the most reliable and robust, but have been previously limited as it has been hard to make inferences about specific alterations in cortical structure and their clinical or functional consequences. Cortical regions can be difficult to segment in elderly brains, so relating cortical changes to a highly reliable measure such as VV has great clinical advantages. Combining information from cortical architecture and ventricular enlargement may allow us to better understand factors affecting normal aging and different stages of neurodegeneration in disease. Future work will also apply the reverse approach, to map summary measures from the cortex (average and change in GM thickness in regions of interest) onto 3D ventricular shapes, to see which ventricular changes are most strongly associated with longitudinal changes in cortical thickness.

References

1. Ferrarini L, et al. Ventricular shape biomarkers for Alzheimer's disease in clinical MR images. Magnetic Resonance in Medicine: Official Journal of the Society of Magnetic Resonance in Medicine. 2008; 59(2):260–267.
2. Qiu A, et al. Regional shape abnormalities in mild cognitive impairment and Alzheimer's disease. Neuroimage. 2009; 45(3):656–661. [PubMed: 19280688]
3. Fjell AM, et al. One-year brain atrophy evident in healthy aging. The Journal of Neuroscience. 2009; 29(48):15223–15231. [PubMed: 19955375]
4. Chou YY, et al. Automated ventricular mapping alignment reveals genetic effects with multi-atlas fluid image in Alzheimer's disease. Neuroimage. 2008; 40(2):615–630. [PubMed: 18222096]
5. Chou YY, et al. Mapping correlations between ventricular expansion and CSF amyloid and tau biomarkers in 240 subjects with Alzheimer's disease, mild cognitive impairment and elderly controls. Neuroimage. 2009; 46(2):394–410. [PubMed: 19236926]
6. Fischl B, Dale AM. Measuring the thickness of the human cerebral cortex from magnetic resonance images. PNAS. 2000; 97(20):11050–11055. [PubMed: 10984517]
7. Apostolova LG, et al. Hippocampal atrophy and ventricular enlargement in normal aging, mild cognitive impairment (MCI), and Alzheimer Disease. Alzheimer Disease and Associated Disorders. 2012; 26(1):17–27. [PubMed: 22343374]
8. Cardenas VA, et al. Comparison of methods for measuring longitudinal brain change in cognitive impairment and dementia. Neurobiology of Aging. 2003; 24(4):537–544. [PubMed: 12714110]
9. Nestor SM, et al. Ventricular enlargement as a possible measure of Alzheimer's disease progression validated using the Alzheimer's Disease Neuroimaging Initiative database. Brain. 2008; 131:2443–2454. [PubMed: 18669512]
10. Jack CR Jr, et al. Comparison of different MRI brain atrophy rate measures with clinical disease progression in AD. Neurology. 2004; 62(4):591–600. [PubMed: 14981176]
11. Ridha BH, et al. Volumetric MRI and cognitive measures in Alzheimer disease: comparison of markers of progression. Journal of Neurology. 2008; 255(4):567–574. [PubMed: 18274807]
12. Wahlund LO, et al. Cognitive functions and brain structures: a quantitative study of CSF volumes on Alzheimer patients and healthy control subjects. Magnetic Resonance Imaging. 1993; 11(2): 169–174. [PubMed: 8455428]

13. Hua X, et al. Optimizing power to track brain degeneration in Alzheimer's disease and mild cognitive impairment with tensor-based morphometry: An ADNI study of 515 subjects. Neuroimage. 2009; 48(4):668–681. [PubMed: 19615450]
14. Paling SM, et al. The application of serial MRI analysis techniques to the study of cerebral atrophy in late-onset dementia. Med Image Anal. 2004; 8(1):69–79. [PubMed: 14644147]
15. Gutman, BA., et al. Shape matching with medial curves and 1-D group-wise registration; 9th IEEE International Symposium on Biomedical Imaging; 2012. p. 716-719.
16. Benjamini Y, Hochberg Y. Controlling the False Discovery Rate - a Practical and Powerful Approach to Multiple Testing. Journal of the Royal Statistical Society Series B-Methodological. 1995; 57(1):289–300.
17. Braak H, Braak E. Neuropathological stageing of Alzheimer-related changes. Acta Neuropathologica. 1991; 82(4):239–259. [PubMed: 1759558]
18. Braskie MN, et al. Plaque and tangle imaging and cognition in normal aging and Alzheimer's disease. Neurobiology of Aging. 2010; 31(10):1669–1678. [PubMed: 19004525]

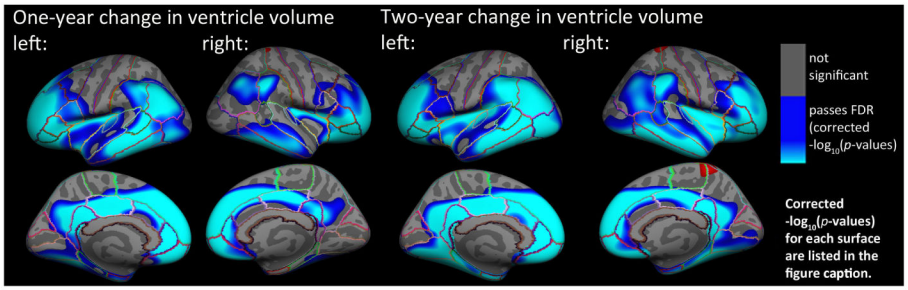

Fig. 1.

Hemispheric 3D maps show significant negative associations in the entire sample between 1-year (N=677) and 2-year (N=536) change in VV and baseline cortical GM thickness in all individuals, after controlling for age, sex, and diagnosis (AD, MCI, or healthy elderly) (1-year change, *left*: $-\log_{10}(p\text{-values})=1.53–3.76$, right: $-\log_{10}(p\text{-values})=1.70–3.96$; 2-year change, left: $-\log_{10}(p\text{-values})=1.51–3.77$, right: $-\log_{10}(p\text{-values})=1.55–3.80$, corrected). Results are corrected for multiple comparisons by thresholding at a q=0.05 false discovery rate (FDR) threshold across the entire brain surface. Blue represents areas where p-values passed the corrected significance threshold for a negative relationship between progressive ventricular enlargement and baseline cortical thickness values (greater VV enlargement associated with lower cortical GM thickness at baseline).

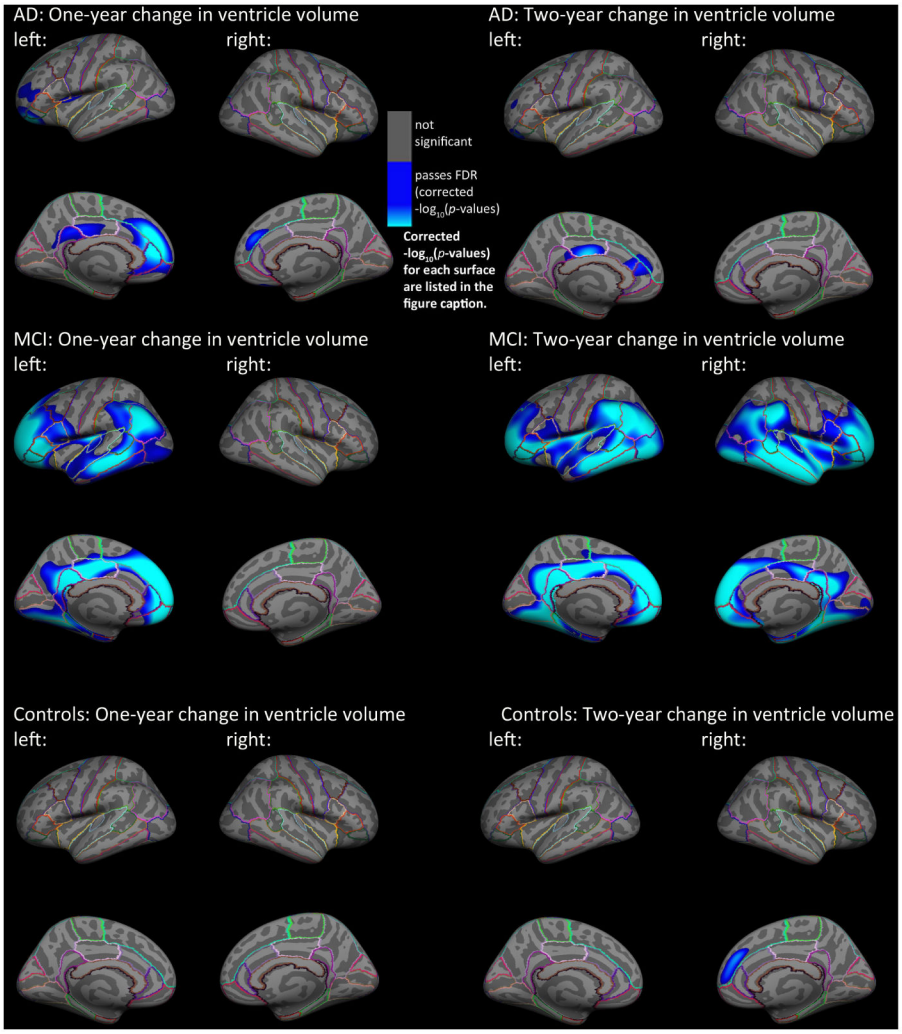

Fig. 2.

Hemispheric 3D maps of significant negative associations between 1-year and 2-year change in VV and baseline cortical gray matter thickness in AD (1-year: N=142; 2-year N: 109), MCI (1-year: N=335; 2-year N: 251), and healthy elderly individuals (1-year: N=200; 2-year N: 176), after controlling for age and sex (AD: 1-year change, left: $-\log_{10}(p\text{-values})=2.39–4.64$, right: $-\log_{10}(p\text{-values})=3.04–5.03$, 2-year change, left: $-\log_{10}(p\text{-values})=2.95–5.20$, right: $-\log_{10}(p\text{-values})=3.64–5.90$; MCI: 1-year change, left: $-\log_{10}(p\text{-values})=1.58–3.84$, right: $-\log_{10}(p\text{-values})=3.28–5.54$, 2-year change, left: $-\log_{10}(p\text{-values})=1.55–3.81$, right: $-\log_{10}(p\text{-values})= 1.55–3.80$; Controls: 1-year change, left: $-\log_{10}(p\text{-values})=1.98–4.24$, right: $-\log_{10}(p\text{-values})=2.36–4.62$, 2-year change, left: $-\log_{10}(p\text{-values})=3.42–5.68$, right: $-\log_{10}(p\text{-values})=3.32–5.58$, corrected). Results were corrected for multiple comparisons by thresholding at a $q=0.05$ false discovery rate (FDR) threshold across the entire brain surface. Blue represents areas where p-values passed the corrected significance threshold for a negative relationship between ventricular enlargement and cortical thickness values (greater VV enlargement associated with lower cortical GM thickness at baseline).

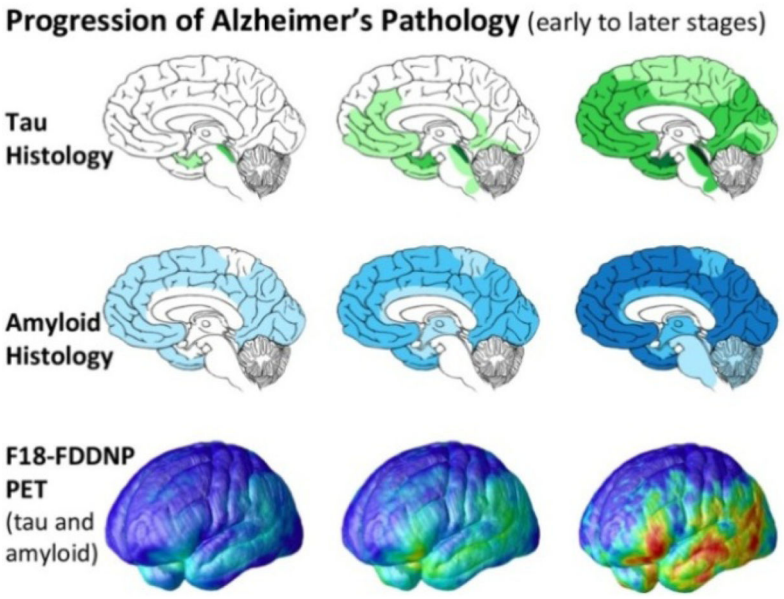

Fig. 3.

Canonical progression of AD pathology (adapted from [17], [18]) as has been mapped previously in non-overlapping elderly samples. These patterns agree well with those seen in our cortical mapping of changes in VV, with significant associations in areas known to be susceptible to AD pathology and no detected relationship in areas that do not have a significant disease burden (primary sensorimotor cortex).

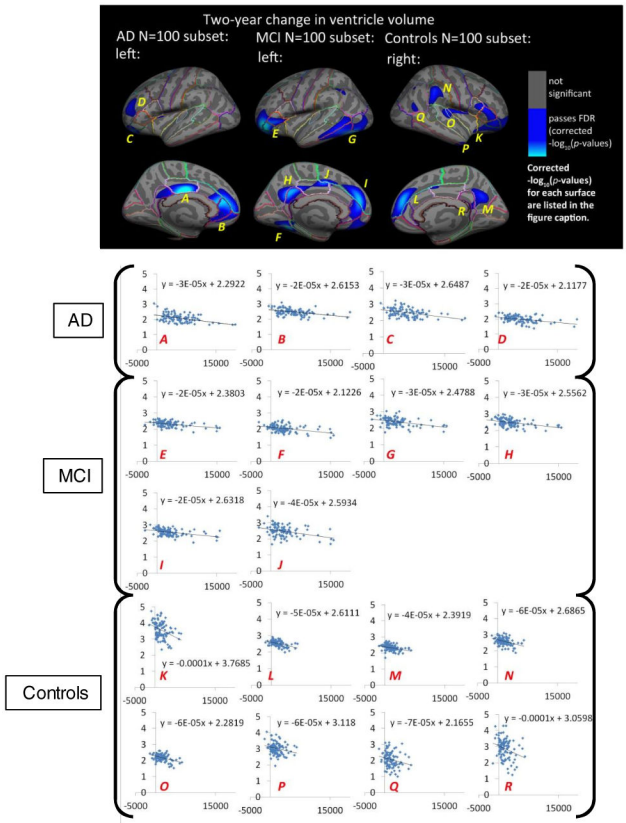

Fig. 4.

Top *Panel:* Hemispheric 3D maps of significant negative associations between 2-year change in VV and cortical GM thickness in matched N=100 sub-samples for AD, MCI, and healthy elderly individuals, after controlling for age and sex (AD: 2-year change, left: $-\log_{10}(p\text{-values})=2.58–4.84$, right: not significant; MCI: 2-year change, left: $-\log_{10}(p\text{-values})=2.15–4.41$, right: not significant; Controls: 2-year change, left: not significant, right: $-\log_{10}(p\text{-values})=2.28–4.54$, corrected). Results are corrected for multiple comparisons by thresholding at a $q=0.05$ false discovery rate (FDR) threshold across the entire brain surface. Blue represents areas where p-values passed the corrected significance threshold for a negative relationship between ventricular enlargement and cortical thickness values (greater VV enlargement associated with lower cortical GM thickness at baseline).

Bottom Panel: Plots of 2-year VV change against mean baseline GM thickness (x-axis: raw 2-year VV change in mm^3, y-axis: mean baseline GM thickness for statistically significant regions in mm). Each data point represents one subject within the matched N=100 subsets for AD, MCI, and healthy elderly control groups (AD: first row, MCI: second and third rows, Controls: last two rows). Each plot represents a distinct and continuous cortical region that passed correction with FDR in the surface GLM maps shown in the top panel of this figure. Within each statistically significant cortical region, GM thickness was averaged across all significant surface vertices. Letters correspond to labels on the cortical surface maps in the top panel and are ordered first by group (AD: A–D; MCI: E–J, controls: K–R)

and then by cortical region (from highest to lowest corrected p-value, all passed FDR in GLMs).